SECRET

TECHNICAL REPORT 178

Copy 085
of 170 Copies
Numbered from 001 thru 170
Consisting of pages i, ii, iii, iv, v and 38 numbered pages.

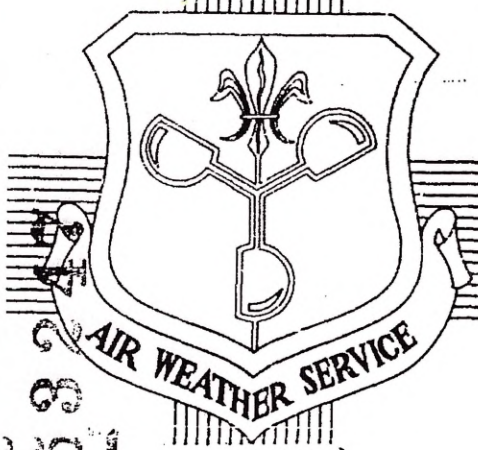

(U) LEAST DISPERSION OF THE MARK 12 RE-ENTRY VEHICLE

By

Karl R. Johannessen

Published By
AIR WEATHER SERVICE (MATS)
UNITED STATES AIR FORCE

September 1964

AWS 2346

04043

SECRET

(U) DISTRIBUTION:

HQ AWS (Incl. stock) [Cys #1-9]
1 Wea Wg [Cys #10-11]
2 Wea Wg [Cys #12-13]
3 Wea Wg [Cys #14-21]
4 Wea Wg [Cys #22-26]
2 Wea Gp [Cys #27-28]
4 Wea Gp [Cys #29-31]
Det 10, Eglin AFB [Cys #32-33]
Det 11, Patrick AFB [Cys #34-35]
Det 21, Edwards AFB [Cys #36-37]
Det 23, Kirtland AFB [Cys #38-39]
Det 24, Holloman AFB [Cys #40-43]
Det 30, Vandenberg AFB [Cys #44-45]
Hq 1210th Sq [Cys #46-50]
8 Wea Gp [Cy #51]
9 Wea R Gp [Cy #52]
AWSWO [Cy #53]
DIA [Cys #54-58]
OAR (RROO) [Cy #59]
OSD (DDR&E/Strat & Def Sys) [Cy #60]
OSD (DDR&E/Mr Sherwin) [Cy #61]
OSD (DDR&E/ARPA) [Cys #62-66]
DDC [Cys #67-86]
Chief, Info. Div., NASA [Cy #87]
HQ USAF (AFGAO) [Cy #88]
HQ USAF (AFCCS) [Cy #89]
HQ USAF (AFRSTA) [Cy #90]
HQ USAF (AFSPD) [Cy #91]
HQ USAF (AFORQ) [Cy #92]
HQ USAF (AFOWX) [Cys #93-94]
AUL (AUL-3T-6633) [Cys #95-96]
AFCRL/CRE [Cy #97]
AFCRL/CREW [Cy #98]
AFCRL/CRH [Cy #99]
AFCRL/CRU [Cy #100]
AFCRL/CRXL [Cy #101]
AFSC (CCSD/G) [Cy #102]
AFSC/For. Techn. Div. [Cy #103]
AFSC/NRD [Cys #104-105]
AFSC/SCGR [Cy #106]
AFSC/SCLS [Cys #107-108]
AFSC/SCLT [Cy #109]
AFSWC (R&D) [Cy #110]
ASD/ASBW [Cys #111-115]
BSD/BSOW [Cys #116-140]
ESD/ESOW [Cys #141-145]
SSD/SSOW [Cys #146-147]

Army Research Office, ATTN: Mrs Whedon, Department of the Army, Washington 25 DC [Cy #148]

Redstone Scientific Information Center, U.S. Army Missile Command, Redstone Arsenal, Ala (ATTN: Chief Document Center) [Cys #149-151]

Commander, Army Ordnance Center, Ballistic Research Laboratory, ATTN: Library, Aberdeen Md [Cy #152]

Chief, Meteorological Branch, Evans Signal Laboratory, Belmar NJ [Cy #153]

U.S. Army Signal Missile Support Agency, ATTN: Mr W Webb, White Sands Missile Range, NMex [Cy #154]

Office of the Naval Weather Service [Cy #155]

Chief of Naval Research, ATTN: Geophysics Branch, Code 1416 [Cy #156]

Director, Naval Research Laboratory, ATTN: Library [Cy #157]

Commander, Naval Ordnance Test Station, Inyokern, Calif [Cy #158]

Commander, Pacific Missile Range (3250), Point Mugu, Calif [Cy #159]

Officer in Charge, Naval Operational Weather Research Facility, Norfolk, Va [Cy #160]

Director, National Security Agency, ATTN: AG Publications, Ft George Meade, Md [Cys #161-163]

(U) DISTRIBUTION:

HQ AWS (Incl. stock) [Cys #1-9]
1 Wea Wg [Cys #10-11]
2 Wea Wg [Cys #12-13]
3 Wea Wg [Cys #14-21]
4 Wea Wg [Cys #22-26]
2 Wea Gp [Cys #27-28]
4 Wea Gp [Cys #29-31]
Det 10, Eglin AFB [Cys #32-33]
Det 11, Patrick AFB [Cys #34-35]
Det 21, Edwards AFB [Cys #36-37]
Det 23, Kirtland AFB [Cys #38-39]
Det 24, Holloman AFB [Cys #40-43]
Det 30, Vandenberg AFB [Cys #44-45]
Hq 1210th Sq [Cys #46-50]
8 Wea Gp [Cy #51]
9 Wea R Gp [Cy #52]
AWSWO [Cy #53]
DIA [Cys #54-58]
OAR (RROO) [Cy #59]
OSD (DDR&E/Strat & Def Sys) [Cy #60]
OSD (DDR&E/Mr Sherwin) [Cy #61]
OSD (DDR&E/ARPA) [Cys #62-66]
DDC [Cys #67-86]
Chief, Info. Div., NASA [Cy #87]
HQ USAF (AFGAO) [Cy #88]
HQ USAF (AFCCS) [Cy #89]
HQ USAF (AFRSTA) [Cy #90]
HQ USAF (AFSPD) [Cy #91]
HQ USAF (AFORQ) [Cy #92]
HQ USAF (AFOWX) [Cys #93-94]
AUL (AUL-3T-6633) [Cys #95-96]
AFCRL/CRE [Cy #97]
AFCRL/CREW [Cy #98]
AFCRL/CRH [Cy #99]
AFCRL/CRU [Cy #100]
AFCRL/CRXL [Cy #101]
AFSC (CCSD/G) [Cy #102]
AFSC/For. Techn. Div. [Cy #103]
AFSC/NRD [Cys #104-105]
AFSC/SCGR [Cy #106]
AFSC/SCLS [Cys #107-108]
AFSC/SCLT [Cy #109]
AFSWC (R&D) [Cy #110]
ASD/ASBW [Cys #111-115]
BSD/BSOW [Cys #116-140]
ESD/ESOW [Cys #141-145]
SSD/SSOW [Cys #146-147]

Army Research Office, ATTN: Mrs Whedon, Department of the Army, Washington 25 DC [Cy #148]

Redstone Scientific Information Center, U.S. Army Missile Command, Redstone Arsenal, Ala (ATTN: Chief Document Center) [Cys #149-151]

Commander, Army Ordnance Center, Ballistic Research Laboratory, ATTN: Library, Aberdeen Md [Cy #152]

Chief, Meteorological Branch, Evans Signal Laboratory, Belmar NJ [Cy #153]

U.S. Army Signal Missile Support Agency, ATTN: Mr W Webb, White Sands Missile Range, NMex [Cy #154]

Office of the Naval Weather Service [Cy #155]

Chief of Naval Research, ATTN: Geophysics Branch, Code 1416 [Cy #156]

Director, Naval Research Laboratory, ATTN: Library [Cy #157]

Commander, Naval Ordnance Test Station, Inyokern, Calif [Cy #158]

Commander, Pacific Missile Range (3250), Point Mugu, Calif [Cy #159]

Officer in Charge, Naval Operational Weather Research Facility, Norfolk, Va [Cy #160]

Director, National Security Agency, ATTN: AG Publications, Ft George Meade, Md [Cys #161-163]

(U) DISTRIBUTION: (Continued)

Central Intelligence Agency, ATTN: OCR Mail Room [Cys #164-168]
The RAND Corporation, ATTN: Planetary Sciences (S Greenfield) [Cy #169]
The RAND Corporation, ATTN: Aero-Astronautics Dept (Mr Lamar) [Cy #170]

(U) CONTENTS

(U) TABLE

(U) LIST OF FIGURES

(U) LIST OF SYMBOLS

(U) Geophysical Parameters

g = Acceleration of gravity.

p = Atmospheric pressure.

ρ = Density of air.

θ = Virtual temperature, degrees Kelvin.

R = Gas constant of dry air.

D = D-value, equal to altitude of a given pressure in actual atmosphere minus altitude of same pressure in standard atmosphere.

z = Altitude above mean sea level.

ω = Non-dimensional pressure

$$\text{variable} = \int_{-\infty}^{p/2P} \exp \xi \, d\ln \xi$$

(U) Re-Entry Vehicle Parameters

W = Weight of re-entry vehicle.

C_D = Drag coefficient.

C_D^* = Hypersonic drag coefficient.

A = Cross section normal to flow.

P = $\sin \alpha_E \, W/C_D A$ = atmospheric pressure at peak deceleration.

(U) Trajectory Parameters

t = Time.

V = Speed of re-entry vehicle.

V_E = Speed at 300,000 feet.

α = Path angle, i.e., angle between horizontal plane and trajectory tangent.

α_E = Path angle at 300,000 feet.

I = Time integral of drag deceleration.

(U) Mathematical, Subscripts, Superscripts, and Indices

$\sigma(x)$ = Standard deviation of x

$$= [\overline{(x - \bar{x})^2}]^{1/2}$$

$\bar{x}$ = Indicates average of x over sample representing locale and month.

$r(x,y)$ = Coefficient of linear correlation between x and y.

$\hat{(\,)}$ = Denotes average with respect to ω along a vertical

$$= (\omega_B - \omega_S)^{-1} \int_{\omega_S}^{\omega_B} (\,) \, d\omega$$

$\delta(\,)$ = Indicates deviation from conditions in standard atmosphere and/or from conditions of ideal behavior of fuzing system components.

$(\,)^*$ = The asterisk indicates that the quantity represents standard atmosphere conditions, and/or programmed behavior of fuzing system components.

$(\,)_B$ = Refers to burst.

$(\,)_S$ = Refers to signal.

$\overline{Ei}(x)$ = Exponential integral

$$= \int_{-\infty}^{x} \exp \xi \, d\ln \xi$$

(U) Fuzing System Parameters

T = Time elapsed between signal and burst.

δT = Error of timer.

ϵ' = Relative error of integrating accelerometer.

September 1964 Technical Report 178

(U) LEAST DISPERSION OF THE MARK 12 RE-ENTRY VEHICLE

1. (U) Introduction

(U) The ever-changing atmosphere causes a dispersion of the trajectories of ballistic re-entry vehicles. Computer programs are in existence which can compute with high precision the trajectories through a given atmosphere. In this manner the effect of the variable atmosphere on the trajectory dispersion may be calculated by solving the re-entry equations for an array of atmospheres which represent the atmospheric variability.

(U) The Monte Carlo method used in conjunction with numerical integration by electronic computers is, however, expensive. The trajectory program presently used at BMD/AFSC costs about $100 per trajectory. As an example, the cost of processing the meteorological data used in this report by Monte-Carlo-ing the trajectories sounding by sounding would have amounted to 1.6 million dollars. The data consists of four years of radiosondes between sea level and 100,000 feet, two soundings per day for two locations and for one month in the summer and one month in the winter, in all, about 1000 soundings. A 16-point change in the trajectory program, varying the burst altitude and one fuzing parameter (the so-called signal altitude, as defined later in the report), brings the cost up to the quoted figure.

(U) Realizing that the Monte Carlo method is not the best way to make use of the vast collection of upper-air data already available in the meteorological archives in processed form, the Air Weather Service has developed an alternate method of assessing the environmental effects. The method, which may be referred to as the perturbation method, has been successfully applied to several re-entry problems [1] [2] [3]. Appendices A and B to this report contain a mathematical précis of the application to the Mark 12 Re-Entry Vehicle.

(U) The following sections define the problem, present the findings, and give conclusions and recommendations for the design of the fuzing system of the Mark 12 Re-Entry Vehicle.

2. (U) The Fuzing Problem of the Mark 12 Re-Entry Vehicle

(U) The object of a fuzing system is to make the warhead detonate at the desired point on the trajectory.

(S) The Mark 12 Re-Entry Vehicle uses an inertial fuzing system. An accelerometer measures the drag deceleration and integrates it over time. When a predetermined value of the integral is reached, a timing device starts counting time at an altitude which in this report is referred to as the signal

altitude. After a predetermined time interval has elapsed, the detonater is activated.

(U) Since the drag deceleration depends on the atmospheric density, variability in the latter will cause a dispersion of the detonation point along the trajectory, with a corresponding dispersion in burst height and range.

(S) The errors of the fuzing components will also contribute to the dispersion. These are mainly the error in the output of the integrating accelerometer and the timing device.

(U) The atmospheric variability and the errors of the fuzing components combine to give the burst dispersion.

(S) The problem which this report deals with, is to define the signal altitude which gives the least dispersion when the system is applied in a given location and season and has a stated level of performance of the fuzing components.

(S) The analysis of the performance of the Mark 12 Re-Entry Vehicle is contained in Appendices A and B. The result of this analysis is that the burst-height error δz_B (positive for a too-high burst) can be written as a linear combination of four sources of errors (equation A-26):

$$\delta z_B = D_B + M\hat{\theta} - N\epsilon - Q\delta T$$

(S) The quantities in the above expression are:

a. (S) M, N, and Q are positive constants for a given burst altitude and signal altitude. Their variation with the altitudes of burst and signal are illustrated in Figures 4, 5, and 6.

b. (S) D_B is the so-called D-value at the programmed burst altitude.

c. (S) $\hat{\theta}$ is the average departure of temperature from nominal values in the layer from signal to burst.

d. (S) ϵ is the relative error (fraction of total value) of the integrating accelerometer.

e. (S) δT is the error of the timing device.

(U) By means of a statistical processing outlined in Appendix B, this expression has been applied to two locations in the U.S.S.R. for one month in summer and one in winter. The results are given in the following section.

3. (U) Burst-Height Errors for Two Locations in the U.S.S.R. in Summer and in Winter

(U) Figure 1 shows the contributions to the variance of the burst-height

error at station 23552 during January. This station is TARK-SALE (64°55'N-77°49'E).

(U) The variance is due to different sources. Panels A, B, D, and E of Figure 1 give the contributions of the four sources in the order they are listed in the previous section.

(S) Panel C shows the contribution due to the correlation of mean temperature and D-value. It is assumed that the co-variance between the errors of the fuzing components (accelerometer, timer) and between these and the meteorological variables are insignificant. There is no reason to assume otherwise.

(S) It is obvious from Figure 1 that the timing error of one millisecond has no practical influence. The other contributions are of similar magnitude, though as is obvious, the meteorological contributions to the variance dominate.

(S) Panel F shows the composite error. A locus of minimum dispersion defines the signal altitude which results in the least dispersion for any given burst altitude between zero and 20,000 feet. For programmed bursts between zero and 7000 feet the optimum signal altitude is about 7000 feet above the burst altitude. For bursts between 7000 feet and 12,000 feet the optimum thickness of the layer from signal to burst shrinks gradually, reaching zero at 12,000 feet. This means that the timer should be dispensed with above 12,000 feet (if practical).

(S) As this example shows, the exact location of the signal altitude in relation to the burst altitude is not very critical. The minimum dispersion (one sigma) is about 430 feet for this location and month for bursts between zero and 5000 feet altitude. Moving the signal altitude up or down 3000 feet from the optimum position would increase the dispersion by only 20 to 30 feet.

(U) Figure 2 shows the burst-height dispersion (one sigma) for the two stations during January and July: 23552, TARK-SALE, U.S.S.R. (64°55'N, 77°49'E) and 38457, TASHKENT, U.S.S.R. (41°16'N, 69°16'E). The results are based on four years of data, 1955-1958, or about 250 soundings for each location and month.

(S) In the four cases the loci of minimum dispersion are all similarly located. It appears that latitudinal and seasonal aspects do not greatly influence the position of the minimum-dispersion curve.

(U) Figure 3 shows the minimum-dispersion curves superimposed on a grid indicating approximately the time of flight between signal and burst. This diagram permits one to compare the minimum-dispersion curves with any programming restrictions placed on the timer.

(S) Observe that a timer setting of three seconds for bursts between zero and 5000 feet and a setting of two seconds for bursts between 5000 feet and

10,000 feet will indicate the least dispersion fairly well.

(U) Figure 3 carries a scale in the right margin which shows approximately the output of the integrating accelerometer in g seconds. Any programming restrictions due to bounds on the output of the accelerometer may be evaluated by means of this scale.

(S) These results, while calculated here for four specific atmospheres, have a more general validity. The D-value and the mean temperature vary in such a fashion, irrespective of season and location, that the signal altitude which gives the least burst-height dispersion, is found 6000 to 7000 feet above the burst altitude for bursts below 10,000 feet.

(S) The results above are predicated on a relative error of the integrating accelerometer of 0.5 percent. A larger value will tend to locate the least-dispersion curve higher up.

4. (U) Conclusions and Recommendations

(U) As a result of this study, the following conclusions have been reached and recommendations are made:

a. (S) The Mark 12 Re-Entry Vehicle will have errors in the burst altitude (and range) which are due to the errors of the fuzing components and to the departure of the atmospheric structure from the particular atmosphere used in the fuzing program.

b. (S) The errors of the fuzing components may be ascribed to the error of the integrating accelerometer (ϵ) and the error of the timing device (δT). Provided that δT is of the order of 20 milliseconds or less, the timer will have no practical influence on the burst-height error. A value of ϵ of 0.5 percent of the total output of the accelerometer will give errors in burst height of the same order of magnitude as the meteorologically induced errors.

c. (S) In order to minimize the burst-height error, the mean atmosphere for the location and month should be used in programming the fuzing system. Otherwise a bias may be introduced which for some targets may amount to as much as 1000 feet in altitude and one-half mile in range.

d. (S) Based on a precision for the accelerometer of 0.5 percent and for the timer of 20 milliseconds or better, the least dispersion in burst altitude is achieved when the signal altitude is chosen 6000 to 7000 feet above the burst altitude. The time of flight from signal to burst with this choice is two to three seconds. This choice is practically independent of season and locale.

e. (S) The minimum-dispersion altitude is not sharply defined. A displacement of the signal altitude upwards from the least-dispersion altitude,

by several thousand feet will not increase the standard deviation of the burst-height error by more than a few tens of feet.

f. (S) As a general conclusion, it can be stated that a choice of signal altitude anywhere between 5000 and 15,000 feet above the burst altitude will give a satisfactory approximation to a least dispersion.

g. (S) The adopted value of ϵ does influence these results. The general effect of an increase of ϵ is to push the least-dispersion signal altitude higher up.

h. (S) With a value of ϵ of 0.5 percent the standard deviation of the burst-height errors will range from about 200 feet to 700 feet, depending on season, location, and burst height.

(U) REFERENCES

[1] Johannessen, Karl R. and Roberts, Charles F.: "(U) Effects of Variable Atmospheric Density on the Deceleration of Re-Entry Vehicles," Air Weather Service Technical Report 155, August 1961 (SECRET)

[2] Johannessen, Karl R.: "(U) Programs for Determining the Minimum Re-Entry Dispersion Due to Atmospheric Variability," Air Weather Service Technical Report 168, May 1963 (SECRET)

[3] Johannessen, Karl R.: "(U) Effects of Atmospheric Variability on the Mark 15 Re-Entry Vehicle Performance," Air Weather Service Technical Report 172, September 1963 (SECRET)

[4] U.S. Standard Atmosphere, 1962: prepared by National Space and Aeronautics Administration, U.S. Air Force, and U.S. Weather Bureau, Superintendant of Documents, U.S. Government Printing Office, Washington 25, D. C., December 1962.

Appendix A

(U) CLOSED-FORM SOLUTION FOR THE BURST ERROR

(U) The Re-Entry Model

(U) When studying the atmospheric perturbations during re-entry it is sufficiently accurate to use an approximate re-entry model. The model used in the present study of the re-entry perturbations is given by the equations:

$$\text{(A-1)} \qquad \frac{dV}{dt} = -\tfrac{1}{2} g\rho \frac{1}{W/C_D A} V^2$$

$$\text{(A-2)} \qquad \alpha = \alpha_E = \text{constant}$$

$$\text{(A-3)} \qquad C_D = C_D^* = \text{constant}$$

The quantities in the equations above are:

- V = speed of vehicle
- t = time
- g = acceleration of gravity
- ρ = air density
- W = vehicle weight
- C_D = drag coefficient
- C_D^* = hypersonic drag coefficient
- A = normal cross section
- α = path angle
- α_E = path angle at entry

(U) While equations (A-1) through (A-3) represent only approximate trajectories, they have sufficient fidelity to be used as basis for a study of the trajectory perturbations caused by atmospheric anomalies.

(U) The method followed in this study is analogous to the method used by the author in several other studies of re-entry problems [1] [2] [3]. The object is to obtain a closed-form expression which relates the re-entry parameter of interest to the atmospheric perturbation variables. In the case of the Mark 12 Re-Entry Vehicle we are interested in the deviations from the programmed burst altitude.

(U) The closed-form expression also points the way to optimization of the fuzing system. By proper selection of the fuzing parameters the burst dispersion can be minimized. As it turns out the selection is dictated by the characteristics of the atmospheric anomalies and by the precision of the

fuzing components.

(U) The Fuzing System in the Mark 12 Re-Entry Vehicle

(S) The Mark 12 fuzing system consists of an integrating accelerometer and a timing device. The integrating accelerometer measures the drag deceleration integrated over time. When a predetermined value of this integral is reached at an altitude we shall name the signal altitude and denoted by subscript S, the timer starts measuring time, and when a certain time interval T has elapsed, the burst mechanism is activated. The event of burst is denoted by the subscript B.

(S) The purpose of this study is to define an optimum fuzing system which selects the value of S for a given B such that the error in the burst altitude caused by the combined effect of atmospheric anomalies and component errors is at a minimum.

(U) The Integral of Drag Deceleration

(S) Equation (A-1) combined with the hydrostatic equation:

$$(A\text{-}4) \qquad -g\rho = \frac{dp}{dz} = \frac{dp}{dt}\frac{dt}{dz}$$

where p is pressure and z altitude, and the kinematic relation:

$$(A\text{-}5) \qquad \frac{dz}{dt} = -V \sin \alpha$$

give

$$(A\text{-}6) \qquad V = V_E \exp(-p/2P)$$

V_E is speed at entry of the atmosphere where $p \approx 0$. The constant

$$(A\text{-}7) \qquad P = \sin \alpha \, W/C_D A$$

which has the dimension of pressure, represents the atmospheric pressure at peak deceleration. For the Mark 12 Re-Entry Vehicle $W/C_D A$ = 2000 lbs per square foot, and with $\alpha = 20°$, 2P becomes 655 mb.

(U) The output of the integrating accelerometer from a threshold value, which for practical purposes may be chosen as zero, to the signal altitude S, may now be written, observing (A-6):

$$(A\text{-}8) \qquad I = \int_{t_E}^{t_S} \frac{dV}{dt}\, dt = V_E - V_S \left[1 - \exp(-p_S/2P)\right]$$

(U) It will be seen from the preceeding equations that the gravity acceleration g sin α has been neglected beside the drag decelerations. However, as we are interested in the environmental perturbations this is of little consequence, as the gravity field remains unaffected by the perturbations.

(U) Time of Flight from Signal to Burst

(U) Returning to equations (A-1) and (A-6) we may write for the time of flight T between the output signal at S to the burst at B:

$$(A\text{-}9) \qquad T = \int_S^B dt = \frac{1}{g \sin \alpha} \int_{p_S}^{p_B} \frac{dp}{\rho V} = \frac{R}{g V_E \sin \alpha} \int_{p_S}^{p_B} \theta \exp (p/2P) \, d\ln p$$

(U) In (A-9) use has been made of the equation of state for moist air:

$$(A\text{-}10) \qquad \rho = \frac{p}{R\theta}$$

where θ is the virtual temperature and R the gas constant for dry air.

(U) We now introduce a new non-dimensional pressure variable, ω, defined by:

$$(A\text{-}11) \qquad d\omega = \exp (p/2P) \, d\ln p$$

or, integrated:

$$\omega = \int_{-\infty}^{p/2P} \exp \xi \, d\ln \xi = \overline{Ei} \, (p/2P)$$

where $\overline{Ei}(x) = \int_{-\infty}^{x} \exp \xi \, d\ln \xi$ is the exponential integral.

(U) Equation (A-9) may now be written:

$$(A\text{-}12) \qquad T = \frac{R}{g V_E \sin \alpha} \int_{\omega_S}^{\omega_B} \theta \, d\omega$$

The limits of the integral are determined from $\omega_S = \overline{Ei} \, (p_S/2P)$; $\omega_B = \overline{Ei} \, (p_B/2P)$.

(U) The relationship in the atmosphere between temperature θ and pressure p or ω is observed by means of radiosondes and rocketsondes. The functional relationship is usually recorded in the form of a trace in some aerological diagram, and it has been found convenient to develop a graphical means of evaluating this trace in terms of the re-entry performance of vehicles. The

so-called Theta-Omega Diagram described in [1] has been constructed for this purpose.

(U) The Perturbation Equation

(U) A re-entry system and its respective fuzing system is programmed to perform in a certain standard atmosphere. For our purpose it is not necessary at this junction to prescribe which standard is to be used. It may, for instance, be the 1962 U.S. Standard Atmosphere [4], or some climatological profile valid for a specific month and location.

(U) The fuzing program is then based on zero errors of the accelerometer and the timing device. Quantities referring to this idealized behavior in a standard atmosphere and with no component error will be denoted by an asterisk.

(U) In the real case the integrating accelerometer will have an error δI defined by:

$$I = I^* + \delta I \tag{A-13}$$

where I^* is the programmed value. In the following it is assumed that δI is roughly proportional to I^*:

$$\delta I = \epsilon I^* \tag{A-14}$$

so that ϵ is a constant which characterizes the instrument.

(U) The error of the timing device δT is defined by:

$$T = T^* + \delta T \tag{A-15}$$

where T^* is the programmed time.

(U) The accelerometer error δI causes a deviation in the pressure at signal altitude which may be computed from equation (A-8). By a variation of equation (A-8) and using (A-14), we find:

$$\delta p_S = 2P \left[\exp\left(p_S^*/2P\right) - 1\right] \epsilon \tag{A-16}$$

(U) In equation (A-16) p_S^* is the pressure at the programmed signal altitude, p_S, the corresponding value in the real case, and δp_S is defined by:

$$p_S = p_S^* + \delta p_S \tag{A-17}$$

(U) Equations (A-15) and (A-12) combine to give:

$$(A\text{-}18)\quad \int_{p_S}^{p_B} \theta \, d\omega - \int_{p_S^*}^{p_B^*} \theta^* \, d\omega - \frac{g\, V_E \sin \alpha}{R} \delta T = 0$$

p_B^* is the programmed pressure at burst, θ^* the virtual temperature in the standard atmosphere, while the quantities without the asterisk again denote the real case.

(U) We further define:

$$(A\text{-}19)\quad \theta = \theta^* + \delta\theta$$

and

$$(A\text{-}20)\quad p_B = p_B^* + \delta p_B$$

(U) Expanding (A-18) and using (A-19) and (A-20) we obtain:

$$(A\text{-}21)\quad \int_{p_S^*}^{p_B^*} \delta\theta \, d\omega + \theta_B^* \, \delta\omega_B - \theta_S^* \, \delta\omega_S - \frac{g\, V_E \sin \alpha}{R} \delta T = 0$$

where we have retained first order terms only, making use of such high-accuracy approximations as the following:

$$\int_{p_B^*}^{p_B} \theta \, d\omega = \theta_B^* \, \delta\omega_B$$

$$\int_{p_S^*}^{p_S} \theta \, d\omega = \theta_S^* \, \delta\omega_S$$

(U) $\delta\omega_B$ and $\delta\omega_S$ are computed from (A-11):

$$\delta\omega_S = \exp\,(p_S^*/2P)\, \frac{\delta p_S}{p_S^*}$$

and from (A-16):

$$(A\text{-}22)\quad \delta\omega_S = 2P \exp\,(p_S^*/2P)\, [\exp\,(p_S^*/2P) - 1]\, \epsilon/p_S^*$$

$$(A\text{-}23)\quad \delta\omega_B = \exp\,(p_B^*/2P)\, \delta p_B/p_B^*$$

(U) The pressure deviation at burst, δp_B, is related to the altitude

deviation δz_B through the hydrostatic equation (A-4). We obtain:

$$(A\text{-}24) \qquad \delta z_B = - \frac{R\,\theta_B^*}{g\,p_B^*}\,\delta p_B + D_B$$

(U) In the last equation, D_B is the so-called D-value at burst altitude. The D-value is defined as the altitude of a given pressure in the real atmosphere minus the altitude of the same pressure in the standard atmosphere. The D-value appears on the right-hand side of equation (A-24) because the geometric measurement of z refers to the ground as a reference, whereas pressure p does not make use of such a reference.

(U) (A-24) together with (A-22) and (A-23) inserted into (A-21) gives us our final equation:

$$(A\text{-}25) \qquad \delta z_B = D_B + \frac{R}{g}\exp\left(-p_B^*/2P\right)\int_{p_S^*}^{p_B^*} \delta\theta\, d\omega$$

$$- \frac{R\,\theta_S^*}{g\,p_S^*}\exp\left(-\frac{p_B^* - p_S^*}{2P}\right)\left[\exp\left(\frac{p_S^*}{2P}\right) - 1\right] 2P\epsilon$$

$$- V_E \sin\alpha \exp\left(-\frac{p_B^*}{2P}\right)\delta T$$

(U) (A-25) relates the deviation in the burst altitude, δz_B, to two meteorological variables plus two fuzing component errors.

a. (U) The meteorological variables are:

(1) (U) The mean temperature deviation between signal and burst, represented by the integral $\int_{p_S^*}^{p_B^*} \delta\theta\, d\omega$

(2) (U) The D-value at burst, D_B.

b. (U) The fuzing component errors are:

(1) (U) The relative error, ϵ, of the output from the integrating accelerometer.

(2) (U) The timing error δT of the device which counts time between signal and burst. [Errors of the detonation-activation mechanism, etc., have been lumped with the timing error.]

(U) Once the signal altitude and the burst altitude have been determined the somewhat involved multipliers for the variables become constants, and we can write:

$$(A\text{-}26) \qquad \delta z_B = D_B + M\,\delta\hat{\theta} - N\epsilon - Q\,\delta T$$

where

$$(A\text{-}27) \qquad \delta\hat{\theta} = \frac{1}{\omega_B^* - \omega_S^*} \int_{p_S^*}^{p_B^*} \delta\theta \, d\omega$$

equals the mean temperature deviation from signal to burst,

$$M = \frac{R}{g} \exp\left(-p_B^*/2P\right)\left(\omega_B^* - \omega_S^*\right)$$

$$N = \frac{2P\,R\,\theta_S^*}{g\,p_S^*} \exp\left(-\frac{p_B^* - p_S^*}{2P}\right)\left[\exp\left(\frac{p_S^*}{2P}\right) - 1\right]$$

$$Q = V_E \sin\alpha \exp\left(-\frac{p_B^*}{2P}\right)$$

Q depends on burst altitude only, M and N on both signal altitude and burst altitude.

(U) In the following the 1962 U.S. Standard Atmosphere [4] will be used as a reference atmosphere. The multipliers M, N, and Q are based on this atmosphere and the D-values also refer to this standard atmosphere.

(U) Figures 7a through 8b show the mean and the standard deviation of the D-value at sea level for the months of January and July. Figures 9 and 10 show the corresponding values at 18,000 feet. For burst altitudes between sea level and 18,000 feet the mean and the standard deviation of the D-value may be obtained by a linear interpolation.

(U) M has been graphed in Figure 4. The units are in feet per degree Celsius.

(U) N is graphed in Figure 5. Units are feet per percent relative accelerometer error.

(S) Q is depicted in Figure 6 in feet per millisecond of error of the timer. As δT is of the order of one millisecond in the Mark 12 Re-Entry Vehicle, it is immediately obvious that the timing error contributes only insignificantly to the over-all error.

(S) If we chose $\epsilon = .5 \times 10^{-2}$ as a representative root-mean-square value of the accelerometer error, it is seen that the D-value and the contributions

of the accelerometer error and the temperature deviation are of comparable magnitude.

(U) Of the various error sources only the meteorological variables are correlated, as there seems to be no reason to assume that the accelerometer error or the timing error depend on each other or on the environment. These relations are explored further in Appendix B.

Appendix B

(U) STATISTICAL DISTRIBUTION OF THE BURST-HEIGHT ERROR

(U) Equation (A-26) of Appendix A gives the burst-height error δz_B as a linear combination of four error sources.

(A-26) $$\delta z_B = D_B + M\,\delta\hat{\theta} - N\epsilon - Q\,\delta T$$

(U) For a given burst altitude and a given signal altitude M, N, and Q are constants.

(U) D_B is the D-value at the nominal burst altitude.

(U) $\delta\hat{\theta}$ is the mean temperature deviation from the nominal value in the layer from signal to burst.

(U) ϵ is the relative error of the integrating accelerometer. In the following calculations a rms-value of $\epsilon = 0.5 \times 10^{-2}$ will be used.

(U) δT is the error of the timing device. A rms-value of $\delta T = 10^{-3}$ second will be used in the following.

(U) We will assume normal distributions of D_B, $\delta\hat{\theta}$, ϵ, and δT, with zero means for ϵ and δT

(U) If the monthly climatological average atmosphere has been used in the programming of the fuzing system, the means of D_B and $\delta\hat{\theta}$ are also zero, and we are only concerned with the dispersion of these quantities about their climatological averages.

(U) Of these four error sources only the atmospheric parameters are likely to have significant correlations.

(U) In the following, $\sigma(x)$ denotes the standard deviation of x:

(B-1) $$\sigma(x) = [\overline{(x - \bar{x})^2}]^{1/2}$$

where the bar indicates averaging over the sample, and $r(x,y)$ denotes the linear correlation between x and y.

(U) With these conventions we obtain from (A-26) for the variance of δz_B:

(B-2) $$\sigma^2(\delta z_B) = \sigma^2(D_B) + M^2\sigma^2(\hat{\theta}) + N^2\sigma^2(\epsilon) + Q^2\sigma^2(\delta T) + 2M\sigma(D_B)\,\sigma(\hat{\theta})\,r(D_B,\hat{\theta})$$

(U) The D-Value at Burst as an Error Source

(U) Figures 7, 8, 9, and 10 show the global distribution of $\sigma(D_B)$ at sea

level and at 18,000 feet for a winter month (January) and a summer month (July). A linear interpolation with altitude will give a good approximation to the value at a burst altitude below 18,000 feet.

(U) Figure 11 shows $\sigma(D_B)$ as a function of altitude for two stations in the U.S.S.R. during summer and winter.

(U) Anomaly of Mean-Layer Temperature from Signal to Burst as an Error Source

(U) Meteorological archives do not as a rule contain statistics on mean-layer temperature, but contain statistics on point values and correlations between point values. This still permits us to calculate the wanted distributions. The methods used are indicated in the following.

(U) From equation (A-27) it follows that:

$$\text{(B-3)} \qquad \sigma^2(\hat{\theta}) = (\omega_B - \omega_S)^{-2} \int_{\omega_S}^{\omega_B} \sigma(\theta_\mu)\, d\mu \int_{\omega_S}^{\omega_B} \sigma(\theta_\zeta)\, r(\theta_\mu, \theta_\zeta)\, d\zeta$$

where the variables μ and ζ are dummies for ω.

(U) For the finite-difference evaluation of (B-3) we proceed as follows: Let the interval from signal to burst contain n data points, of which the signal and burst altitudes are two points, as indicated in Figure 12. To each point is ascribed a value of ω and $\sigma(\theta)$; and the correlation coefficient $r(\theta_i, \theta_j)$ for any pair of points is known.

(U) When each temperature sounding in the sample is approximated by straight-line segments between the tabulated data points, we obtain for the distribution (B-3):

$$\text{(B-4)} \qquad \sigma^2(\hat{\theta}) = (\omega_B - \omega_S)^{-2} \sum_{i=1}^{n} \sum_{j=1}^{n} \sigma(\theta_i)\, \sigma(\theta_j)\, r(\theta_i, \theta_j)\, k_i k_j$$

where the K's are given by:

$$k_1 = (\omega_2 - \omega_1)/2$$

$$k_n = (\omega_n - \omega_{n-1})/2$$

$$k_i = (\omega_{i+1} - \omega_{i-1})/2; \quad i = 2, 3, \ldots (n-1)$$

(U) Figure 13 shows $M^2\sigma^2(\hat{\theta})$ for the two stations in U.S.S.R. during January and July. Figure 11 shows $\sigma(\theta)$ as a function of altitude.

(U) The Integral Accelerometer as an Error Source

(U) We will assume

$$\sigma(\epsilon) = .5 \times 10^{-2}$$

and further

$$r(D_B, \epsilon) = r(\hat{\theta}, \epsilon) = r(\delta T, \epsilon) = 0$$

(U) Figure 5 shows twice the error due to this effect.

(U) The Timing Device as an Error Source

(U) A value

$$\sigma(\delta T) = 10^{-3} \text{ second}$$

gives the contribution illustrated in Figure 6.

(U) Errors Due to Correlation of Mean Temperature and D-Value

(U) The last term in equation (B-2) contains $r(D_B, \hat{\theta})$ which has to be evaluated by special technique due to the same reasons as indicated for $\sigma(\hat{\theta})$.

(U) From the definition of the vertical average, given in Appendix A:

$$\hat{x} = (\omega_B - \omega_S)^{-1} \int_{\omega_S}^{\omega_B} x \, d\omega$$

combined with the classical definition of the correlation coefficient

$$r(x,y) = [\sigma(x)\ \sigma(y)]^{-1}\ \overline{xy}$$

we obtain, after some calculation:

$$\text{(B-5)} \qquad r(D_B, \hat{\theta}) = [\sigma(\hat{\theta})\ (\omega_B - \omega_S)]^{-1} \int_{\omega_S}^{\omega_B} \sigma(\theta)\ r(D_B, \theta)\ d\omega$$

(U) Using the same finite-difference scheme as before (Figure 12), we can write:

$$\text{(B-6)} \qquad r(D_B, \hat{\theta}) = [(\omega_B - \omega_S)\ \sigma(\hat{\theta})]^{-1} \sum_{i=1}^{n} k_i\ \sigma(\theta_1)\ r(D_B, \theta_1)$$

(U) Figure 14 shows the last term in equation (B-2) for the two selected locations in summer and winter.

(U) The Dispersion of the Burst Height

(U) From each of the error sources discussed above, we may construct the distribution of the total error and its dependence on the altitudes of signal and burst. Figures 1 and 2 show the result of our calculations for the four atmospheres chosen as examples. In the six panels of Figure 1, panels A, B, C, D, and E show the contributions from each of the terms in equation (B-2) to the variance of δz_B. Panel F shows the standard deviation of the burst error and represents the final result of our calculations.

(U) Figure 2 shows the end result for all four atmospheres. Table 1 contains the results in tabular form.

TABLE 1 (S)

Contribution to Variance [Columns A, B, C, and D × 10^{-4} (feet)^2] and Standard Deviation of the Burst-Height Error [F (feet)]. (a) Station 38457, July; (b) 38457, January; (c) Station 23552, July; (d) 23552, January; S is signal altitude; B is burst altitude.

		Column A				Column B				Column C				Column D	Column F			
	S, mb	(a)	(b)	(c)	(d)	(a)	(b)	(c)	(d)	(a)	(b)	(c)	(d)		(a)	(b)	(c)	(d)
B = 1000 mb	1000	0.77	1.37	4.00	14.43	0	0	0	0	0	0	0	0	10.62	337	346	382	500
	850	0.77	1.37	4.00	14.43	0.34	0.61	0.67	0.62	0.51	0.14	1.74	0.78	4.89	255	265	336	455
	700	0.77	1.37	4.00	14.43	1.96	2.39	4.98	1.67	0.94	0.14	3.84	2.02	2.13	241	246	387	450
	500	0.77	1.37	4.00	14.43	5.42	5.05	7.07	5.60	1.25	0.15	5.51	2.62	0.72	286	270	416	483
	300	0.77	1.37	4.00	14.43	5.73	6.77	5.33	6.26	1.14	0.21	4.25	1.93	0.23	281	293	372	478
	200	0.77	1.37	4.00	14.43	7.36	6.41	4.81	5.68	0.87	0.45	5.82	0.83	0.14	302	289	384	459
	100	0.77	1.37	4.00	14.43	7.36	6.41	4.81	5.68	0.87	0.94	5.82	0.83	0.08	301	297	384	458
B = 850 mb	850	0.77	1.37	5.07	15.05	0	0	0	0	0	0	0	0	7.57	289	299	356	476
	700	0.77	1.37	5.07	15.05	0.34	0.61	0.67	0.62	0.51	0.14	1.74	0.78	3.38	224	235	330	445
	500	0.77	1.37	5.07	15.05	1.96	2.39	4.98	1.67	0.94	0.15	3.84	2.02	1.14	219	225	388	446
	300	0.77	1.37	5.07	15.05	5.42	5.05	7.07	5.60	1.25	0.21	5.51	2.62	0.37	279	265	424	486
	200	0.77	1.37	5.07	15.05	5.73	6.77	5.33	6.26	1.14	0.45	4.25	1.93	0.23	281	297	386	484
	100	0.77	1.37	5.07	15.05	7.36	6.41	4.81	5.68	0.87	0.94	5.82	0.83	0.13	302	297	398	466
B = 700 mb	700	0.81	4.41	7.07	16.00	0	0	0	0	0	0	0	0	5.29	247	311	352	461
	500	0.81	4.41	7.07	16.00	1.11	1.06	1.60	1.44	0.62	2.15	4.65	3.10	1.80	208	307	389	473
	300	0.81	4.41	7.07	16.00	4.99	3.93	5.56	4.53	1.29	3.92	8.40	4.75	0.58	277	358	465	509
	200	0.81	4.41	7.07	16.00	6.82	6.12	4.96	4.95	1.60	4.44	6.57	3.97	0.36	310	312	435	503
	100	0.81	4.41	7.07	16.00	8.66	6.62	7.40	4.84	1.72	4.77	0.51	2.73	0.20	337	400	390	488
B = 500 mb	500	2.86	5.29	15.37	21.05	0	0	0	0	0	0	0	0	3.27	248	293	432	493
	300	2.86	5.29	15.37	21.05	3.16	1.90	2.35	2.01	4.11	4.60	9.46	5.10	1.06	335	478	531	541
	200	2.86	5.29	15.37	21.05	7.46	2.88	4.80	1.10	5.90	5.47	6.02	3.72	0.65	411	378	518	515
	100	2.86	5.29	15.37	21.05	9.13	7.80	3.98	2.70	5.58	5.22	-6.62	-0.40	0.37	424	432	362	487

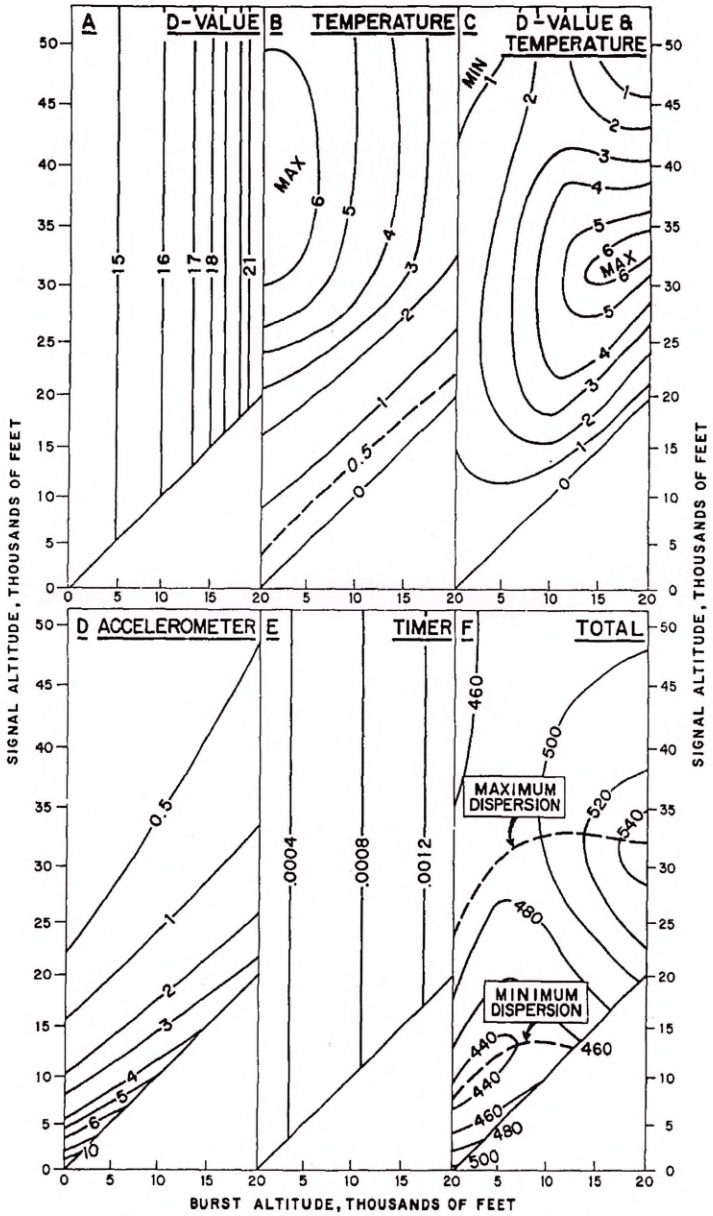

**CONTRIBUTIONS TO VARIANCE (A,B,C,D,E,(FEET)^2 x 10^{-4})
AND STANDARD DEVIATION OF BURST HEIGHT ERROR (F,Feet)
STATION 23552, JANUARY**

Figure 1. (S)

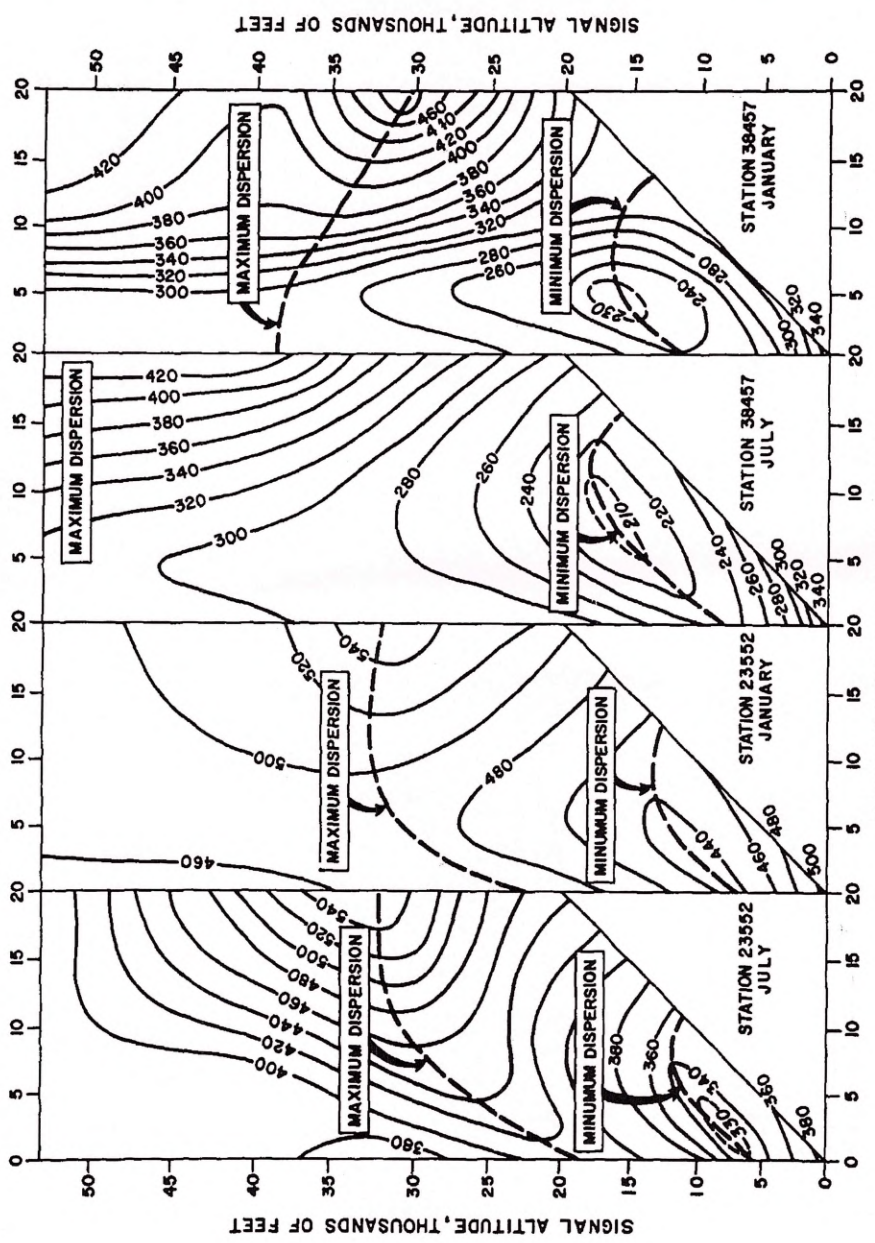
SIGNAL ALTITUDE, THOUSANDS OF FEET
STATION 38457 JANUARY
STATION 38457 JULY
STATION 23552 JANUARY
STATION 23552 JULY
MAXIMUM DISPERSION
MINIMUM DISPERSION
BURST ALTITUDE, THOUSANDS OF FEET
STANDARD DEVIATION OF BURST ERROR, FEET
(FOUR YEARS DATA: 1955-1958)

Figure 2. (S)

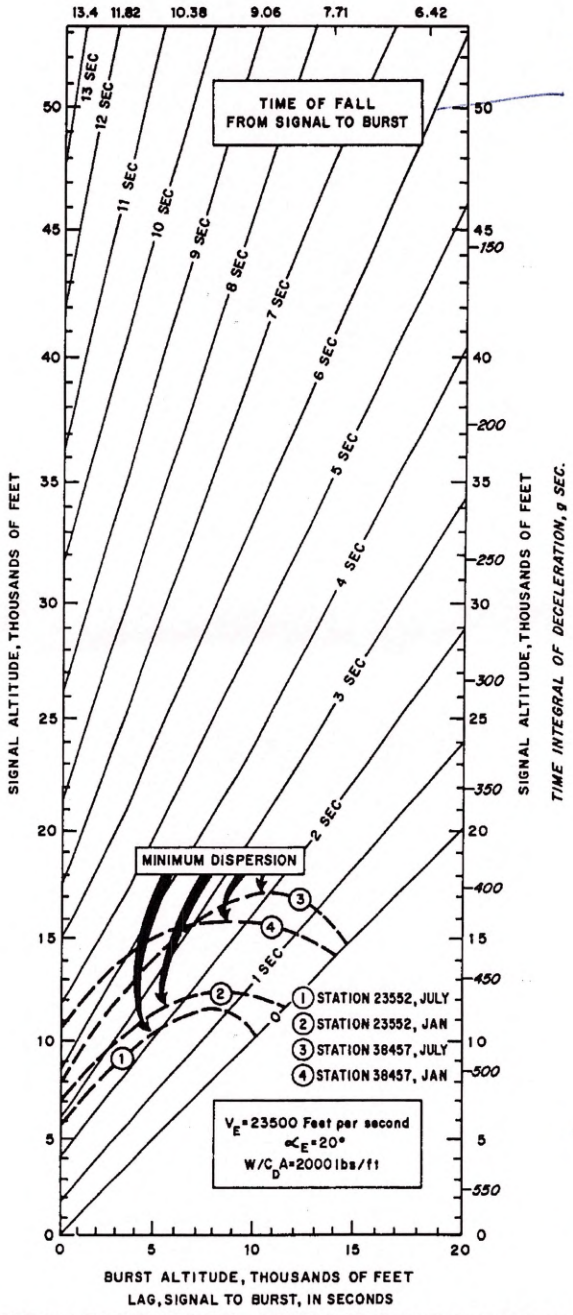

MINUMUM DISPERSION AGAINST TIME OF FLIGHT

Figure 3. (S)

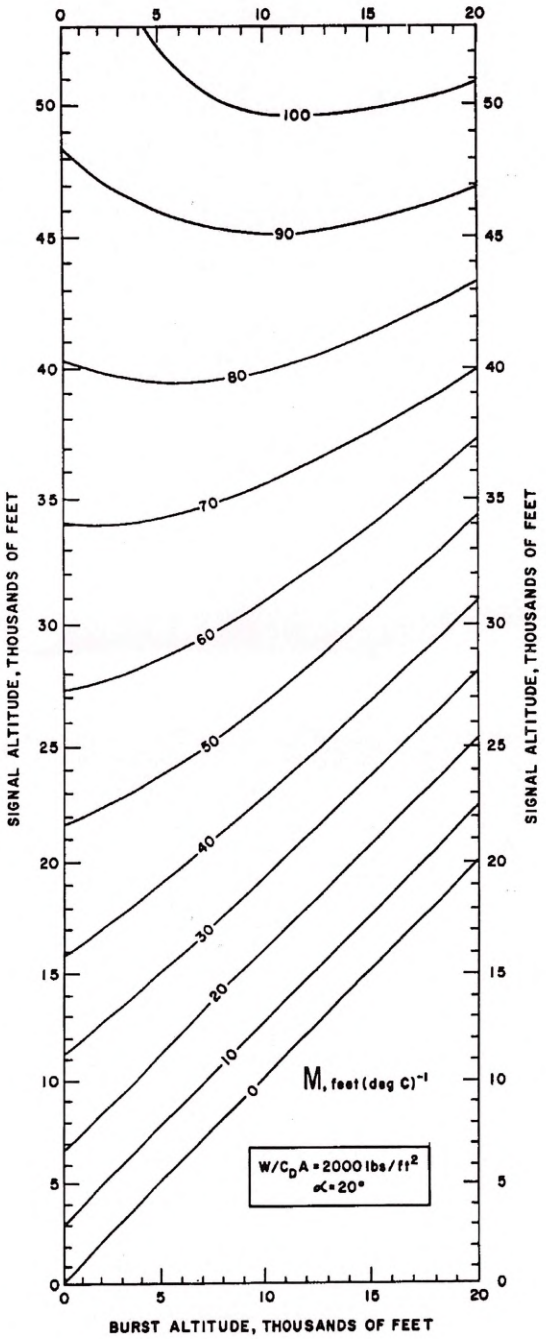
SIGNAL ALTITUDE, THOUSANDS OF FEET
BURST ALTITUDE, THOUSANDS OF FEET
100
90
80
70
60
50
40
30
20
10
0
M, feet (deg C)⁻¹
W/C_D A = 2000 lbs/ft²
α = 20°

Figure 4. (S)

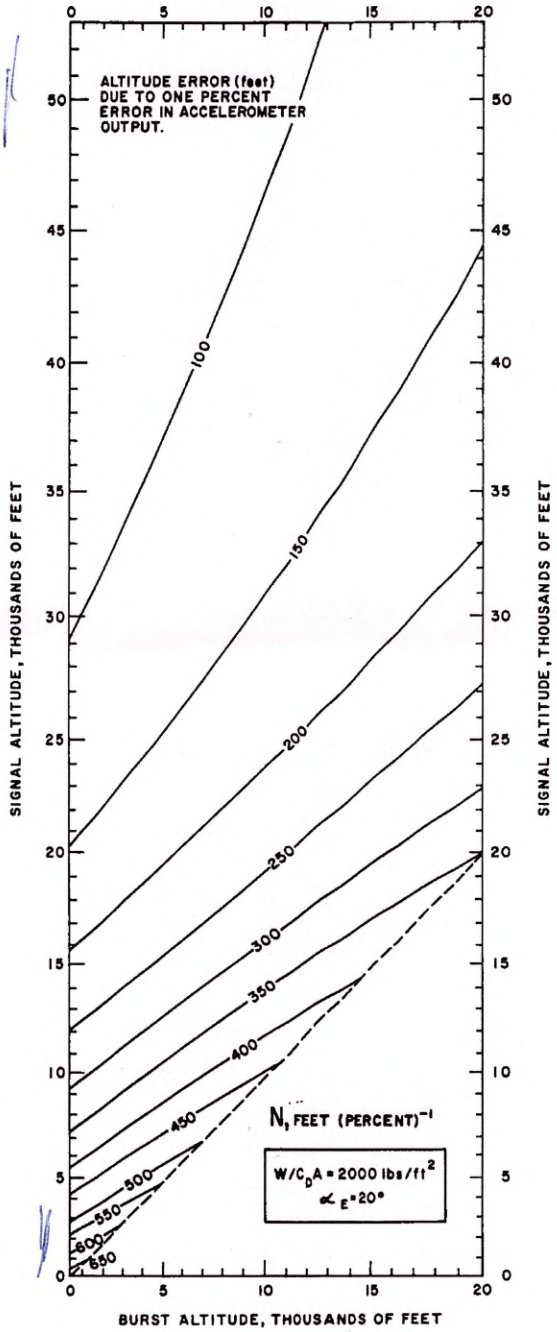
ALTITUDE ERROR (feet) DUE TO ONE PERCENT ERROR IN ACCELEROMETER OUTPUT.
100
150
200
250
300
350
400
450
500
550
600
650
N, FEET (PERCENT)⁻¹
W/C_DA = 2000 lbs/ft²
α_E = 20°
SIGNAL ALTITUDE, THOUSANDS OF FEET
SIGNAL ALTITUDE, THOUSANDS OF FEET
BURST ALTITUDE, THOUSANDS OF FEET
0
5
10
15
20
25
30
35
40
45
50

Figure 5. (S)

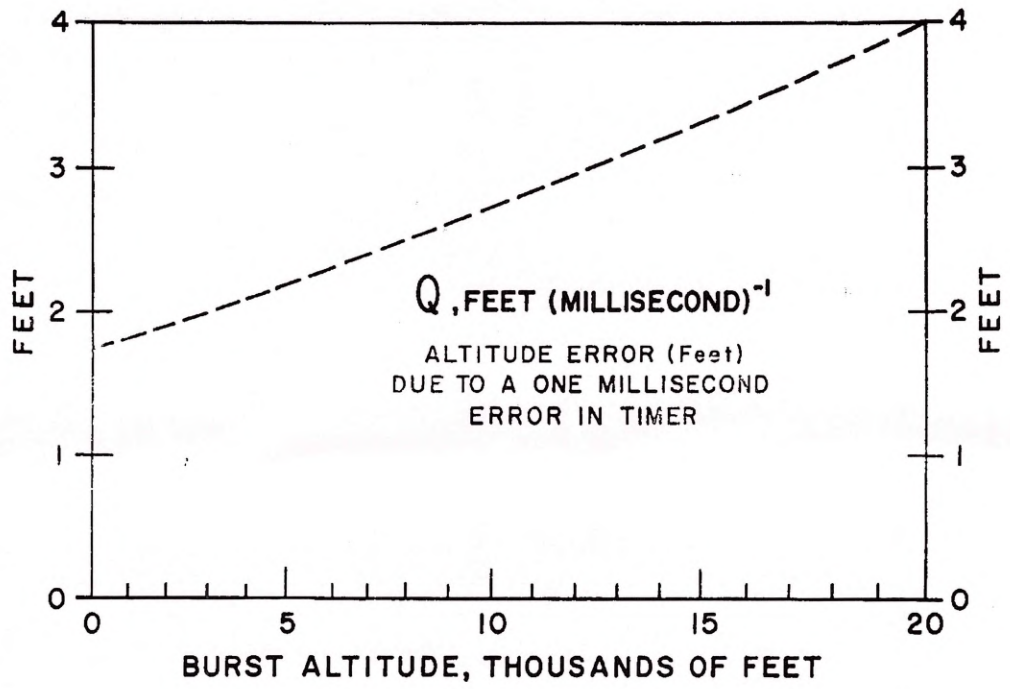
4
3
2
1
0
FEET
Q , FEET (MILLISECOND)⁻¹
ALTITUDE ERROR (Feet)
DUE TO A ONE MILLISECOND
ERROR IN TIMER
0
5
10
15
20
BURST ALTITUDE, THOUSANDS OF FEET

Figure 6. (S)

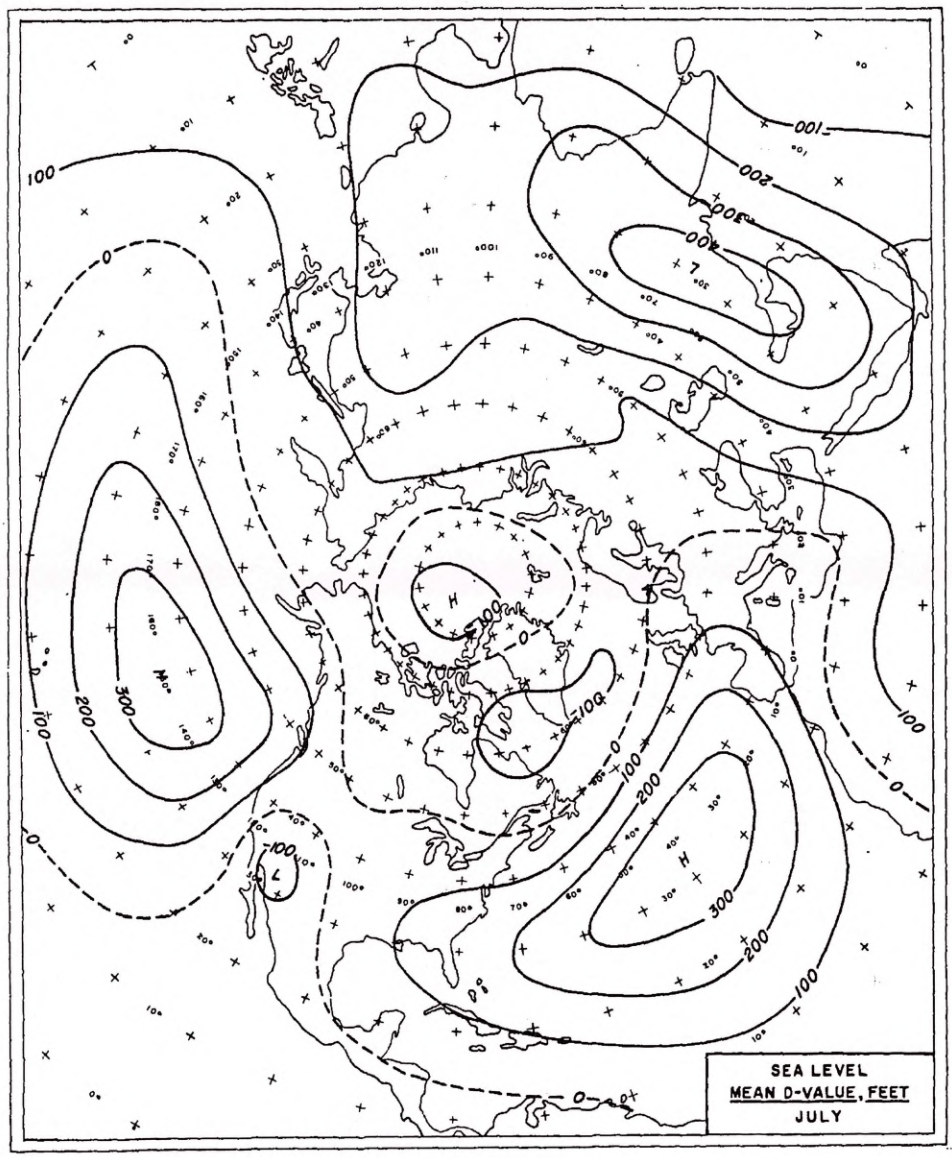

Figure 7a. (U)

(This page is unclassified)

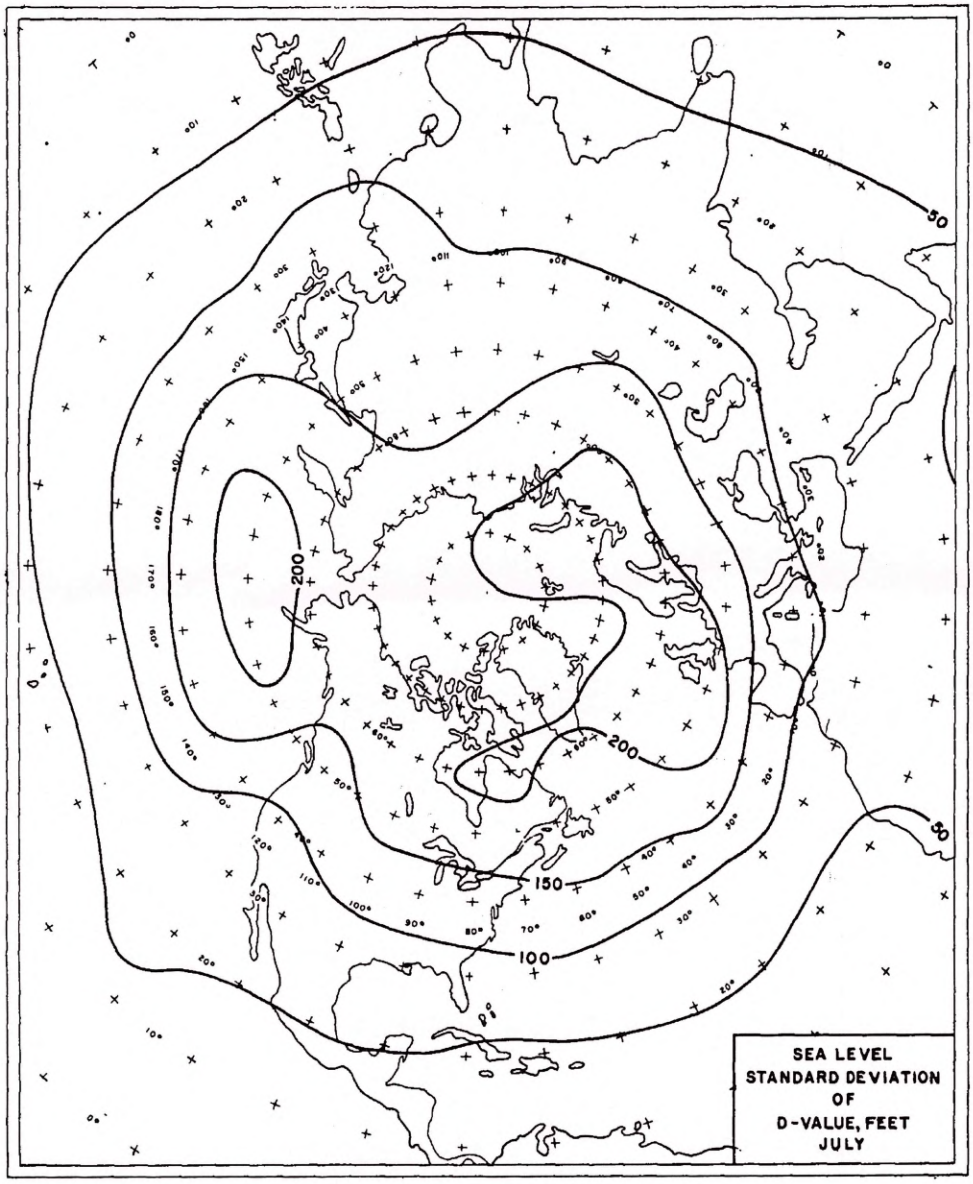
50
200
200
150
100
50
SEA LEVEL
STANDARD DEVIATION
OF
D-VALUE, FEET
JULY

Figure 7b. (U)

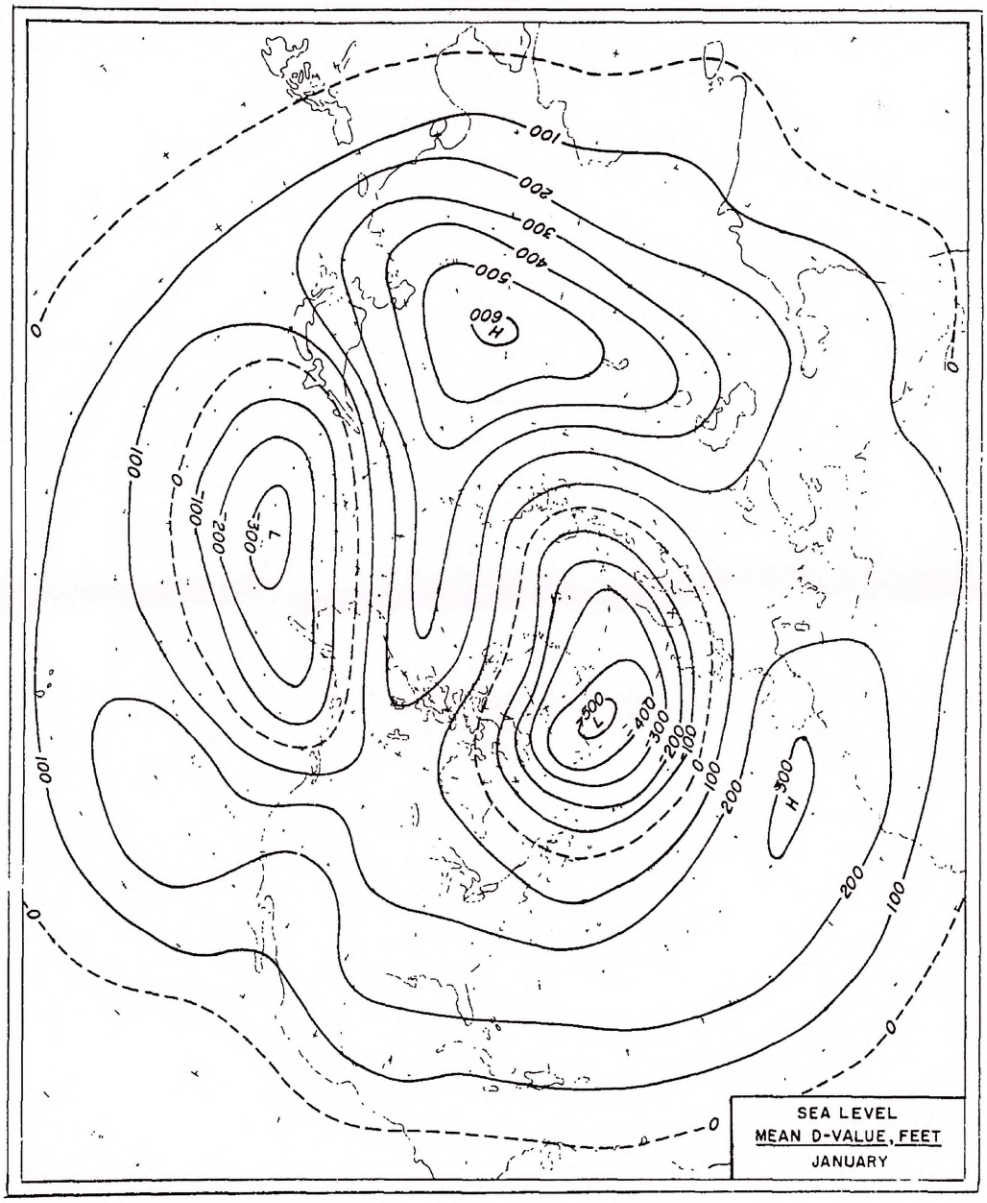

Figure 8a. (U)

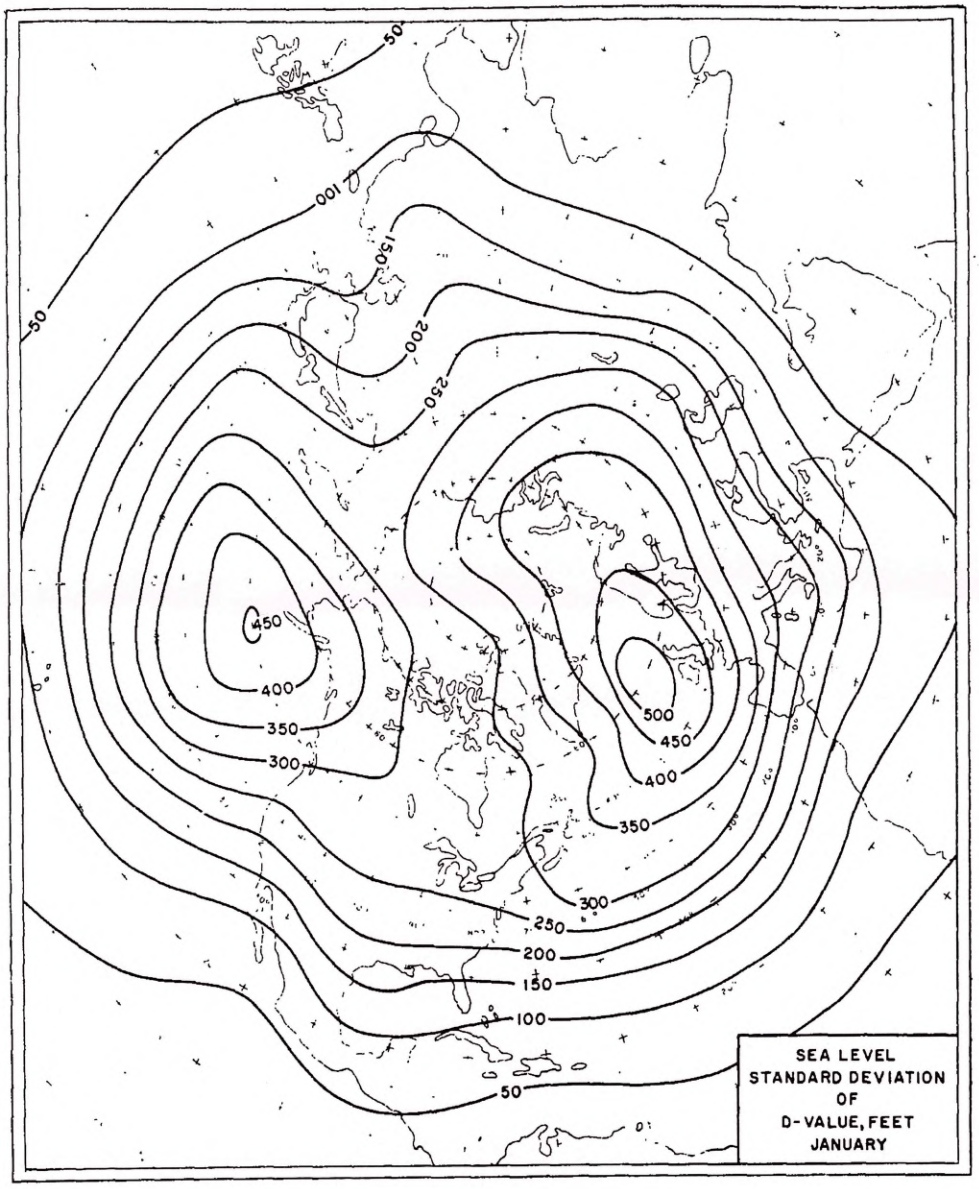
50
100
150
200
250
300
350
400
450
500
SEA LEVEL
STANDARD DEVIATION
OF
D-VALUE, FEET
JANUARY

Figure 8b. (U)

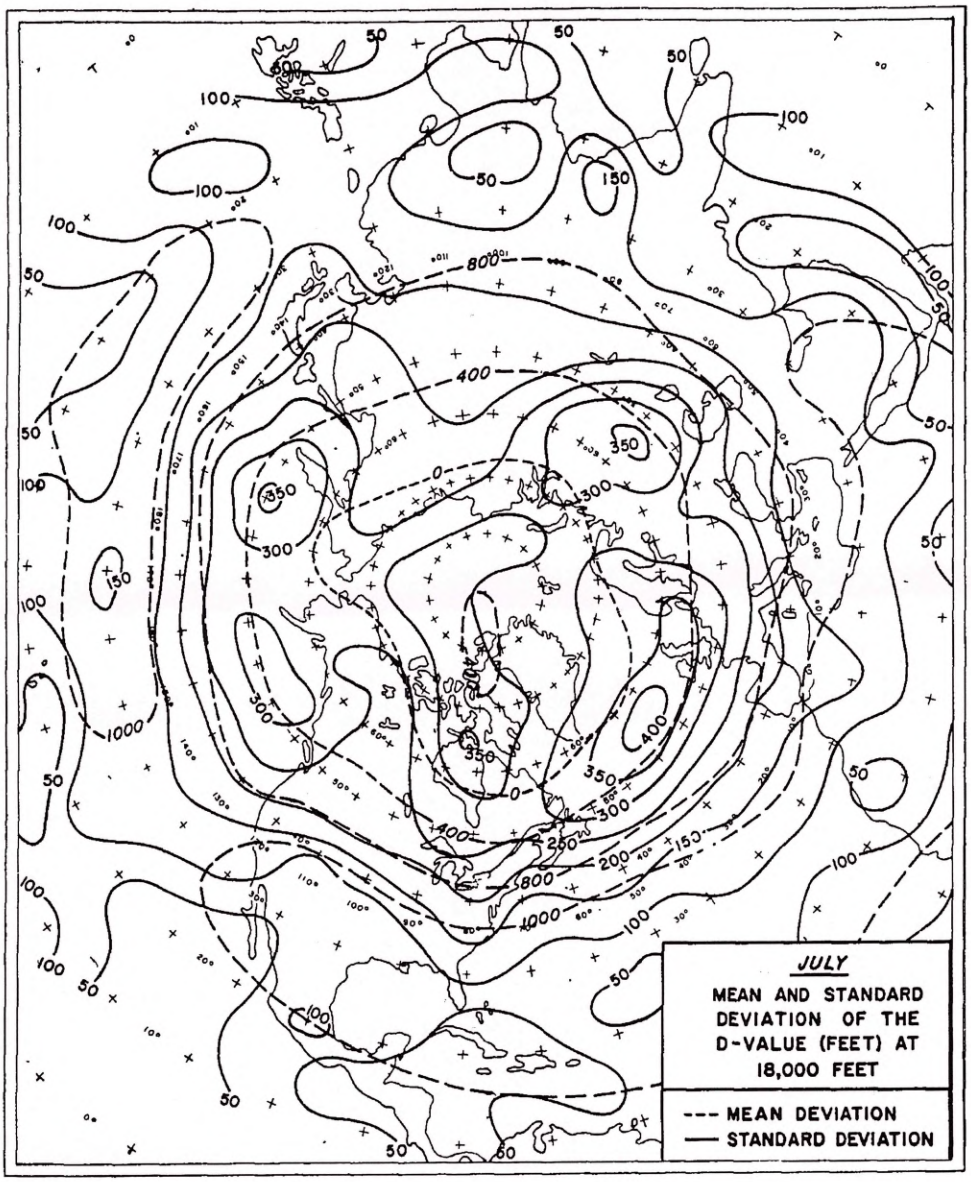
JULY
MEAN AND STANDARD DEVIATION OF THE D-VALUE (FEET) AT 18,000 FEET
--- MEAN DEVIATION
— STANDARD DEVIATION

Figure 9. (U)

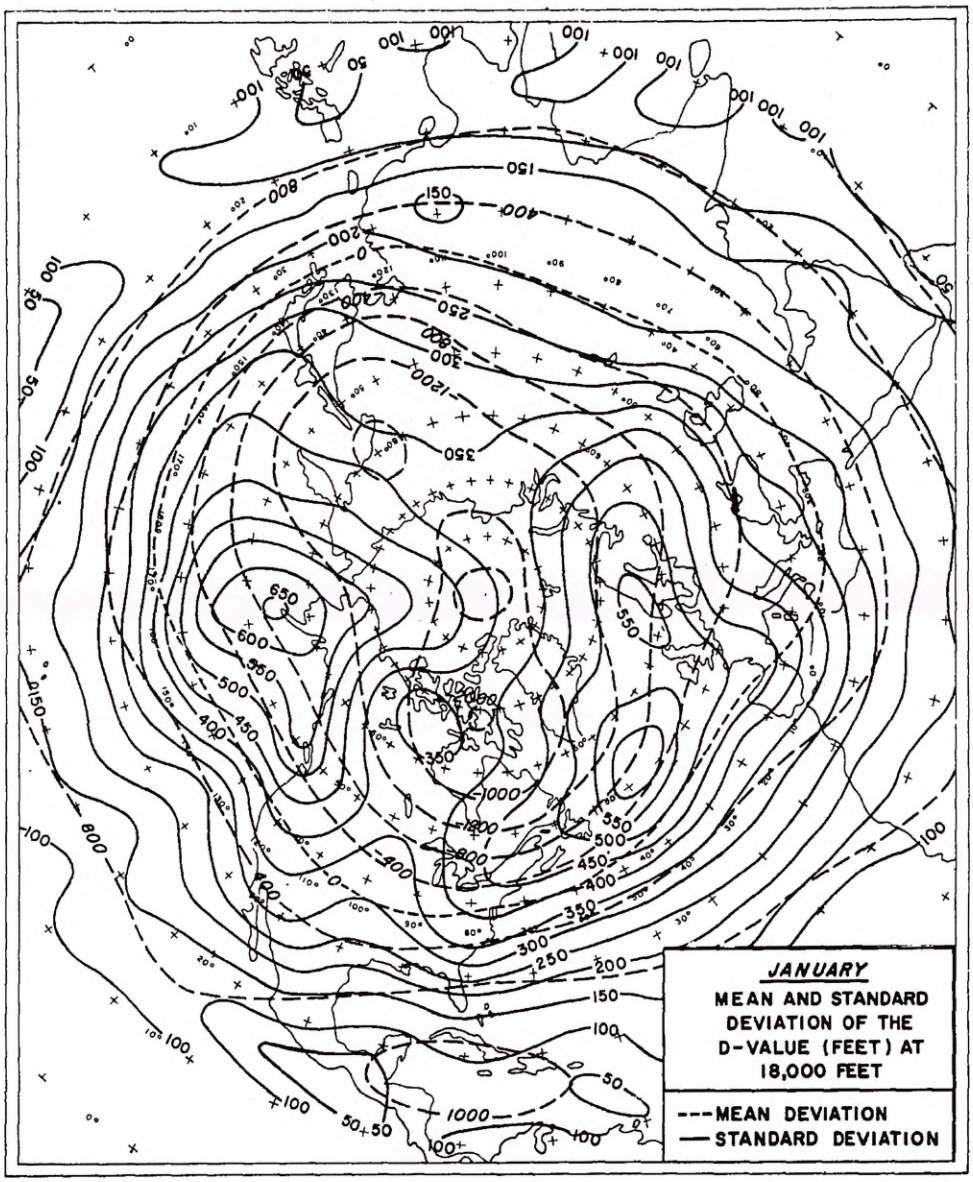
JANUARY
MEAN AND STANDARD DEVIATION OF THE D-VALUE (FEET) AT 18,000 FEET
---MEAN DEVIATION
—STANDARD DEVIATION

Figure 10. (U)

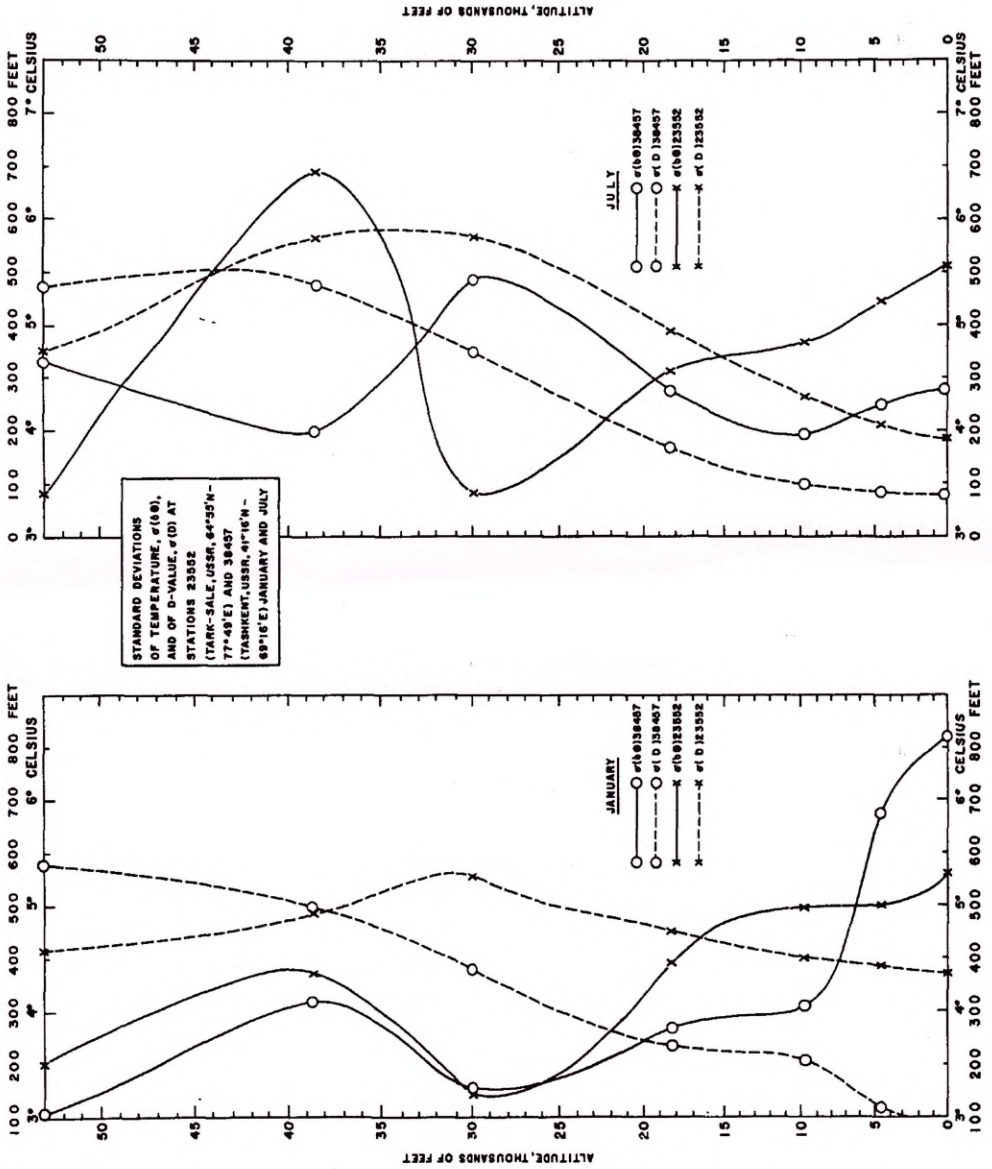
STANDARD DEVIATIONS OF TEMPERATURE, σ(t0), AND OF D-VALUE, σ(D) AT STATIONS 23552 (TARK-SALE, USSR, 64°55'N-77°49'E) AND 38457 (TASHKENT, USSR, 41°16'N-69°16'E) JANUARY AND JULY
JULY
JANUARY
ALTITUDE, THOUSANDS OF FEET
CELSIUS
FEET

Figure 11. (U)

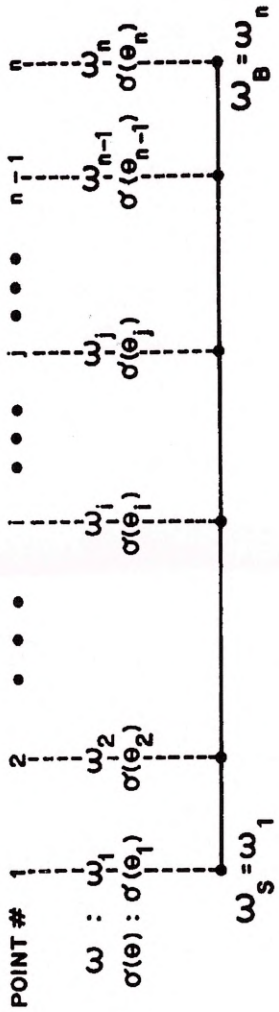

FINITE DIFFERENCE NOTATION

Figure 12. (U)

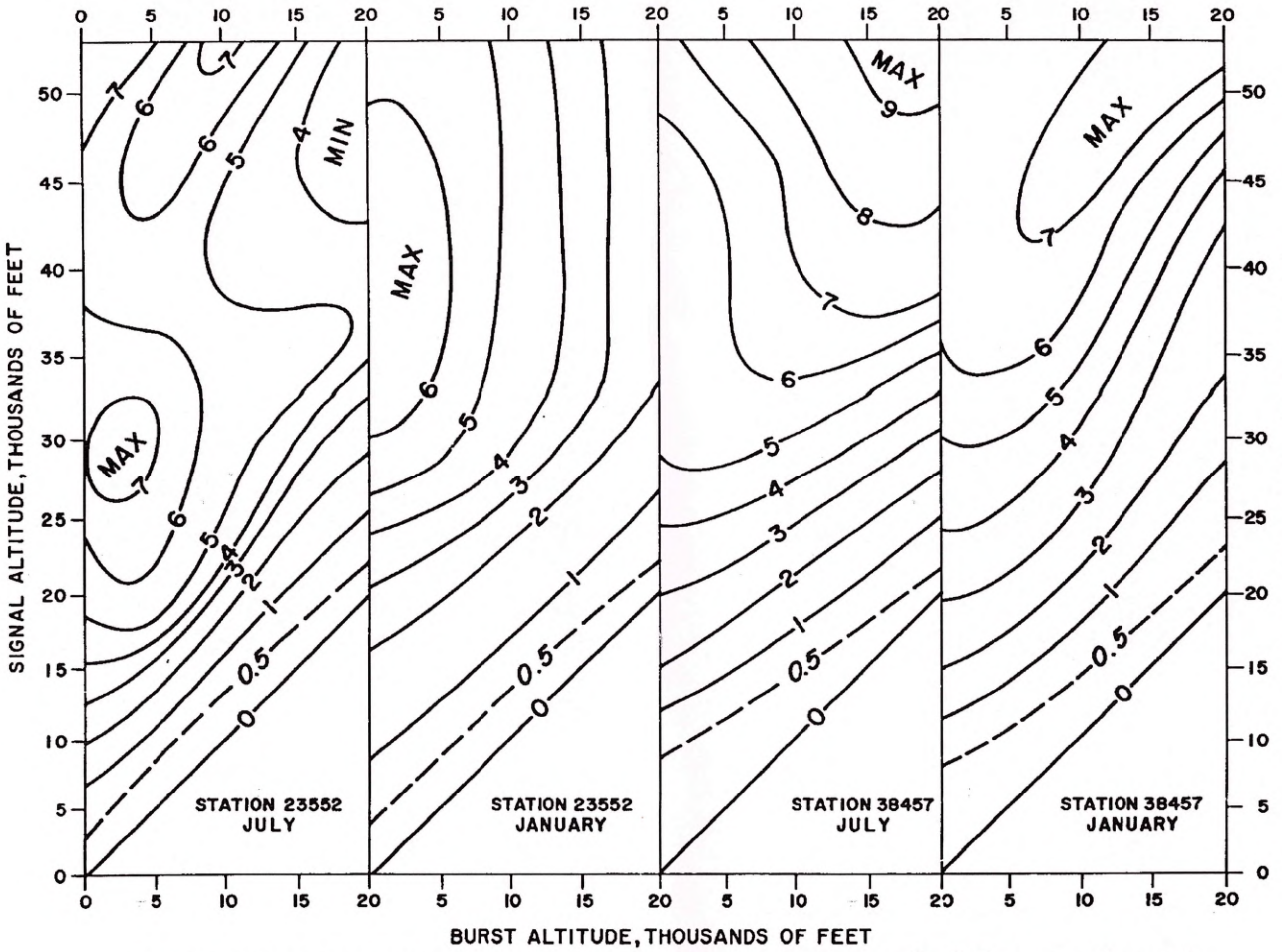
SIGNAL ALTITUDE, THOUSANDS OF FEET
BURST ALTITUDE, THOUSANDS OF FEET
STATION 23552 JULY
STATION 23552 JANUARY
STATION 38457 JULY
STATION 38457 JANUARY
MAX
MIN
MEAN TEMPERATURE CONTRIBUTION TO VARIANCE, $M^2\sigma^2(\hat{\theta})$, (feet)^2 x 10^{-4}

Figure 13. (S)

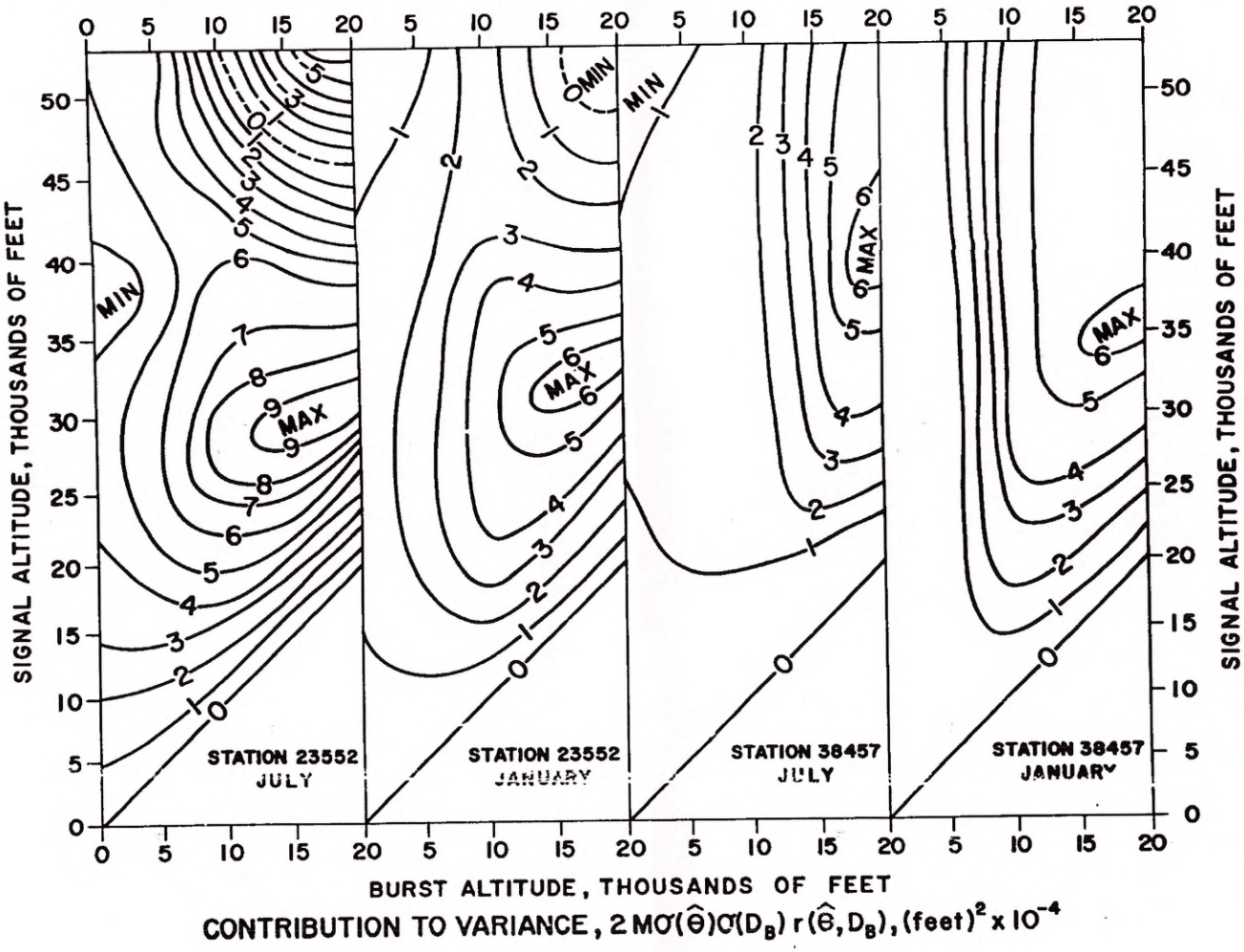
SIGNAL ALTITUDE, THOUSANDS OF FEET
SIGNAL ALTITUDE, THOUSANDS OF FEET
STATION 23552
JULY
STATION 23552
JANUARY
STATION 38457
JULY
STATION 38457
JANUARY
MIN
MAX
BURST ALTITUDE, THOUSANDS OF FEET
CONTRIBUTION TO VARIANCE, $2M\sigma(\hat{\theta})\sigma(D_B)\,r(\hat{\theta}, D_B)$, (feet)$^2 \times 10^{-4}$

Figure 14. (S)